Electronic Supplementary Material (ESI) for Organic & Biomolecular Chemistry
This journal is © The Royal Society of Chemistry 2011

# *Supporting Information*

## Novel Organogelators Based on Amine-derived Hexaazatrinaphthylene

Daniel García Velázquez,[a] Alejandro González Orive,[b] Alberto Hernández Creus,[b,] Rafael Luque and
Ángel Gutiérrez Ravelo[a,]*

[a] *Instituto Universitario de Bio-Orgánica "Antonio González", Universidad de La Laguna, C/ Astrofísico Francisco Sánchez, 2, 38206 La Laguna, Tenerife, Spain*

[b] *Departamento de Química Física, Facultad de Química, Universidad de La Laguna, Campus de Anchieta s/n. 38206, Spain.*

agravelo@ull.es ahcreus@ull.es

### - Contents list -

## 1. Experimental Section: General Remarks.

### *1.1. Compound Synthesis and Characterization:*

$^1$H and $^{13}$C NMR spectra were obtained on a Bruker Advance400 instrument. IR spectra were obtained on a Bruker IFS 66 instrument with ATR accessories or on a Bruker IFS 28/55 instrument using KBr pellets at room temperature, recording the spectrum directly operating at 8 cm$^{-1}$ resolution with 40 scans. Corrections were made for the solvent. Melting point was measured in a Büchi Melting Point B-540 apparatus and is uncorrected. Chromatographic purifications were conducted by column chromatographic using 0.063–0.2 mm silica gel obtained from Fluka. TLC analysis was facilitated by the use of UV light (254 nm) with fluorescent-indicating plates (silica gel on aluminum, Sigma). Microwave heating was performed in a commercial single-mode microwave CEM Discover oven. MALDI-TOF MS were conducted on a Bruker BIFLEX III time-of-flight (TOF) mass spectrometer (Bruker Daltonics, Billerica, MA, USA) operated in a positive ion reflection mode at 20 kV accelerating voltage, where the samples were dissolved in DMSO (200 μg/μl) and diluted in water to obtain 0.1% DMSO. In all experiments 0.5 μl of 2,5-Dihydroxybenzoic acid (DHB; 5 mg/ml) was spotted on the MALDI target (600 mm Anchorchip$^{TM}$; Bruker-Daltonics) and air-dried, then 1 μl of sample solution was layered on top of the matrix and air-dried. For one main spectrum, 30 subspectra with 30 shots *per* subspectrum were accumulated. The profiling spectra were calibrated externally with a premix calibration kit (Bruker Daltonic) and the standard mass deviation was less than 10 ppm. Solvents used were dried by standard distillation procedures[1] or were of p.a. grade and purchased from Aldrich. Commercially available reagents were used without further purification.

### *1.2. Transmission Electron Microscopy (TEM):*

The TEM images were obtained as follow: 1–2 μL of the gel suspension was allowed to adsorb for 3–5 minutes onto copper grids (300 mesh) coated with both formvar and silicon monoxide. A Teflon sheet was used to remove the excess of solvent by a slight contact with the sample (x2) allowing the formation of a thinner film on the grid. The specimens were finally dried at low pressure (>10$^{-5}$ Torr) for 24 h before taking the electronic pictures. The relatively large size of the gel pieces made negative staining unnecessary for visualization. Samples were observed with a Jeol JEM 1010 transmission electron microscope operating at a voltage of 90 kV. In studying the specimens, we first searched for patches of the gel to be sure that the observed structures originate from the gel. Micrographs were taken from structures at the periphery of the gel patches because here the fibers are deposited in a layer thin enough to be observed by transmission electron microscopy.

### *1.3. Scanning Electron Microscopy (SEM):*

Scanning Electron Microscopy (SEM) images were taken from TEM gel samples coated with Au at a working distance of 50 mm under 30 mA electric current for 80 seconds obtaining a film thickness *ca.* 9-12 nm (19.3 g/cc gold deposition). The coated grids were observed with a Jeol JSM 6300 scanning electron microscope operating at an accelerating voltage of 20 kV.

### *1.4. Atomic Force Microscopy (AFM):*

Atomic force microscopy (AFM) imaging was performed in air with a Nanoscope IIIa microscope from Digital Instruments (Veeco). Commercial Pt-Ir tips (TAP150A 126-169 KHz) were used for AFM measurements, respectively. In the case of AFM imaging, the tips used because of their low values of spring constant and oscillating frequencies implies a very soft interaction with samples.

### *1.5. Nuclear Magnetic Resonance (NMR):*

A warmed solution of LMWOG **1** in DMSO-$d_6$ was rapidly transferred into a NMR-tube via a syringe. Upon cooling a homogeneous gel was obtained.

### *1.6. Gelation Experiments:*

A weighted amount of LMWOG and the appropriate solvent were placed in a screw-capped glass vial (3 cm length and 0.5 cm diameter) and heated with a heat-gun until the solid was completely dissolved (isotropic solution). The resulting clear solution was cooled down to room temperature and left for 15 min, after which time the state of the solution was monitored visually by turning the test vial upside-down. The material was classified as “gel” if it did not exhibit gravitational flow.

***1.6.1. Estimation of Gel-to-Sol Phase Transition Temperature (*$T_{gel}$*).*** Gelation temperatures were determined by the “dropping ball method”:[2] A glass ball (40 mg) was placed on the surface of the gel and the tube sealed. The sample was placed in a stirred thermostated oil bath. The temperature was raised at a rate of *ca.* 1 ºC min$^{-1}$, while the position of the glass ball was observed and the temperature simultaneously monitored with the aid of thermocouple in one of the vials. Here, the melting point of a particular sample ($T_{gel}$) was defined as the temperature at which the glass ball begins falling down. The experimental error of $T_{gel}$ was less than 1 ºC.

### *1.7. Differential Scanning Calorimetry (DSC):*

A given amount of gel was placed in a preweighted pan, which was sealed and weighted on a six-decimal plate balance. Heating and cooling scans were measured on a Pyris Diamond DSC (Perkin Elmer) instrument at a scan of 10 ºC min$^{-1}$. After the measurements the pan was weighted again to check for possible leakage.

### *1.8. Rheology:*

Oscillatory rheology experiments (DTS, DFS, and DSS) were performed with an AR 2000 rheometer (TA Instruments), which were reproducible in random replicates. The loss (G'') and elastic (G') moduli were measured in the linear viscoelastic regime.

## 2. Synthesis of compounds

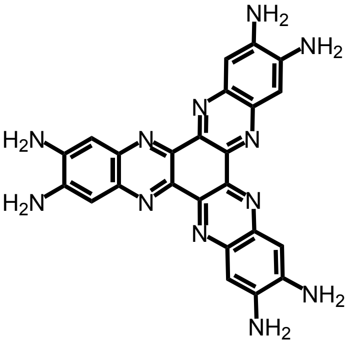

**2.1 5,6,11,12,17,18-hexaazatrinaphthylene-2,3,8,9,14,15-hexaamine (G1)**: Experimental procedure reported in literature[13]

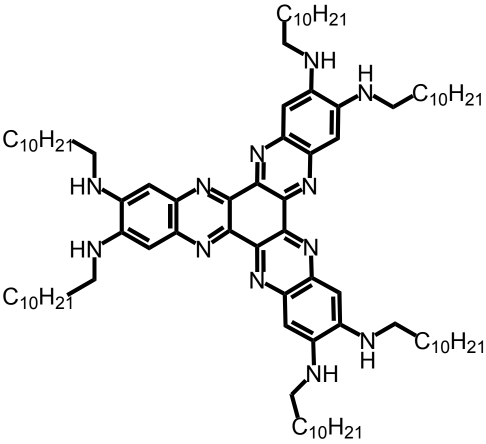

### 2.2 2,3,8,9,14,15-hexaundecyldiquinoxalino[2,3-a:2',3'-c]phenazine-2,3,8,9,14,15-hexaamine (1):

To a 10 mL reaction vial was added G1 (30 mg, 0,06 mmol) and 1-bromoundecane (12 equiv, 160 µL, 0,72 mmol) followed by 0.5 mL of water miliQ®. The closed vessel was heated and stirred in CEM Discover reaction cavity for 30 min at 150 ºC. Then the reaction vessel was rapidly cooled at 60 ºC. Upon cooling, the mixture was diluted with water (5 mL), neutralized with $NaHCO_3$, and extracted with EtOAc (3 x 10 mL); the organic phase was evaporated under reduced pressure, and the residue was purified by flash silica gel column chromatography (30% EtOAc in *n*-hexane as eluent). Drying for 48 h (under vacuum, 5-10 mmHg, 60-80 ºC) afforded a green-dark solid as pure product (66 mg, 78%).

**Aspect**: green-dark solid

**$^1$H NMR (400 MHz, *d6*-DMSO, δ ppm):** 0.78 (18H, t), 1.15-1.21 (96H, m), 1.68 (12H, m), 3.18 (12H, t), 6.73 (6H, s)

**$^{13}$C NMR (100 MHz, *d6*-DMSO, δ ppm):** 14.4, 23.57, 25.75, 26.62, 27.50, 28.37, 29.68, 30.77, 32.95, 33.82, 51.28, 127.88, 132.90, 137.04, 137.92

**FT-IR (DCM)**: 3419, 2527, 2254, 1576, 1472, 1231, 1025, 825, 764 cm$^{-1}$

**UV-vis (c = 10$^{-4}$ M, EtOH):** 343 (log ε 3.84), 242 (3.99), 203 (4.11)

**MS MALDI-TOF (*m/z* %)**: 1399.73 [M$^+$]

**Elemental analysis:** for $C_{90}H_{150}N_{12}$: 1400.23 g/mol. Calcd (%): C: 77.20, H: 10.80, N: 12.00. Found (%): C: 77.20, H: 10.78, N: 12.02.

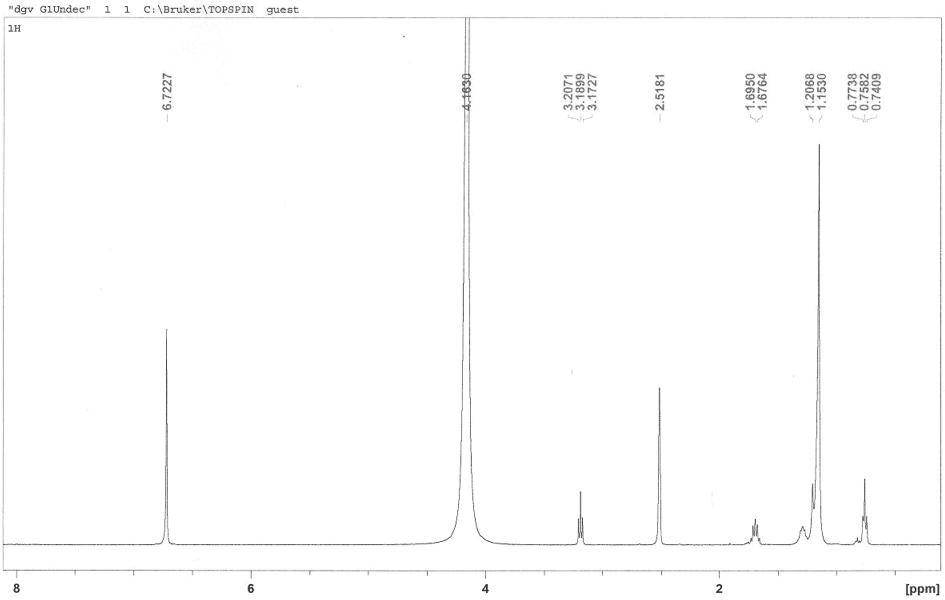

**Figure S1.** $^1$H NMR for **1** in DMSO-$d_6$

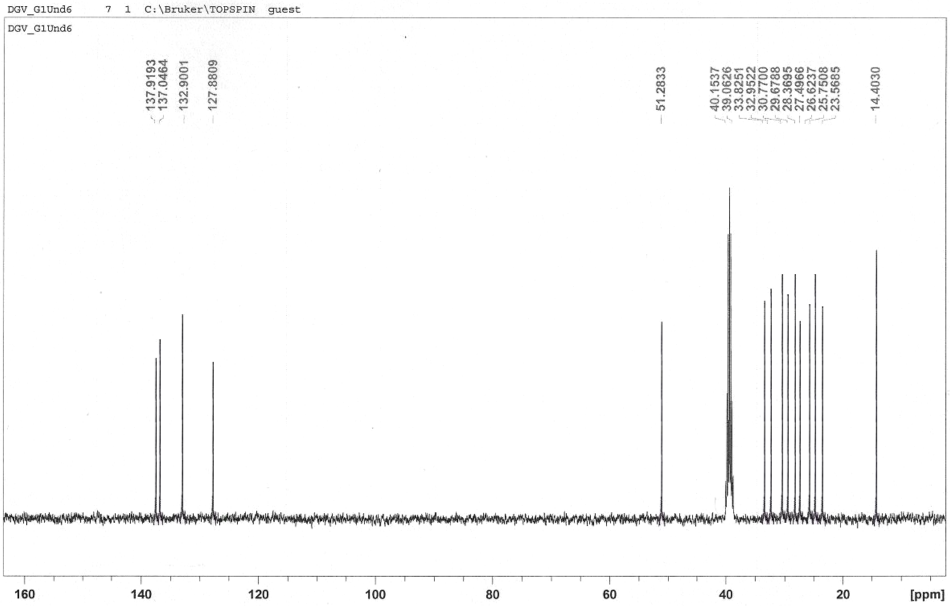

**Figure S2.** $^{13}$C NMR for **1** in DMSO-$d_6$

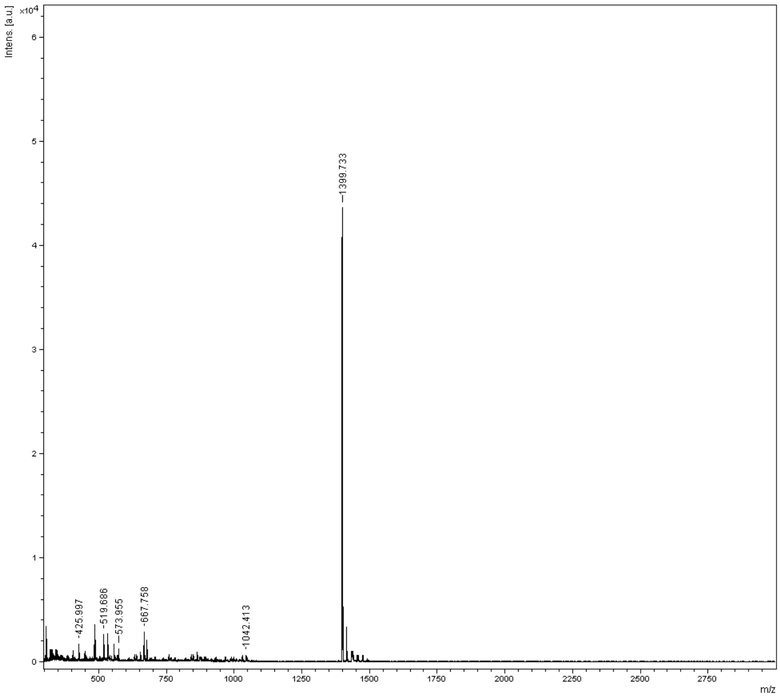

**Figure S3.** MALDI-TOF for **1** (DHB matrix; 5 mg/ml)

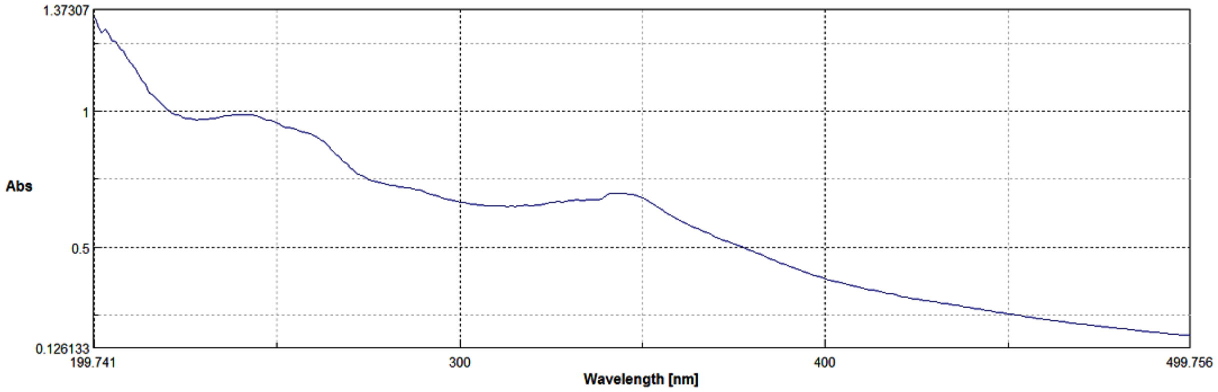

**Figure S4.** UV-vis spectra for compound **1** in EtOH ($10^{-4}$M)

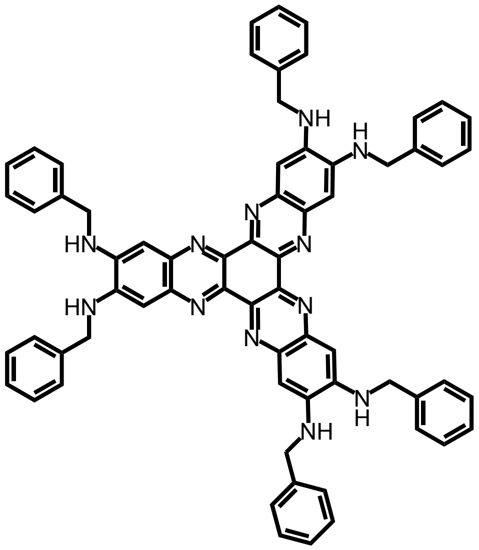

## 2.3 2,3,8,9,14,15-hexabenzyldiquinoxalino[2,3-a:2',3'-c]phenazine-2,3,8,9,14,15-hexaamine (2):

To a 10 mL reaction vial was added G1 (30 mg, 0,06 mmol) and benzyl bromide (12 equiv, 86 μL, 0,72 mmol) followed by 0.5 mL of water miliQ®. The closed vessel was heated and stirred in CEM Discover reaction cavity for 30 min at 150 ºC. Then the reaction vessel was rapidly cooled at 60 ºC. Upon cooling, the mixture was diluted with water (5 mL), neutralized with $NaHCO_3$, and extracted with EtOAc (3 x 10 mL); the organic phase was evaporated under reduced pressure, and the residue was purified by flash silica gel column chromatography (50% EtOAc in *n*-hexane as eluent). Drying for 48 h (under vacuum, 5-10 mmHg, 60-80 ºC) afforded a red solid as pure product ( 58 mg, 96%).

**Aspect**: red solid
**$^{1}$H NMR (400 MHz, *d6*-DMSO, δ ppm):** 4.28 (12H, s), 6.79 (6H, s), 7.29-7.41 (30H, $CH_{aromatic\ benzylic}$)
**$^{13}$C NMR (100 MHz, *d6*-DMSO, δ ppm):** 49.34, 125.25, 126.25, 127.45, 128.65, 133.65, 137.44, 138.24, 140.24
**FT-IR (EtOH)**: 3345, 2928, 2852, 1582, 1568, 1426, 1369, 1282, 1158, 1017, 830, 769 cm$^{-1}$
**UV-vis (c = 10$^{-4}$ M, EtOH):** 346 (log ε 3.72), 240 (3.99), 201 (4.12)
**MS MALDI-TOF (*m/z* %)**: 1014.88 [M$^{+}$]
**Elemental analysis:** for $C_{66}H_{54}N_{12}$: 1015.22 g/mol. Calcd (%): C: 78.08, H: 5.36, N: 16.56. Found (%): C: 78.04, H: 5.64, N: 16.84.

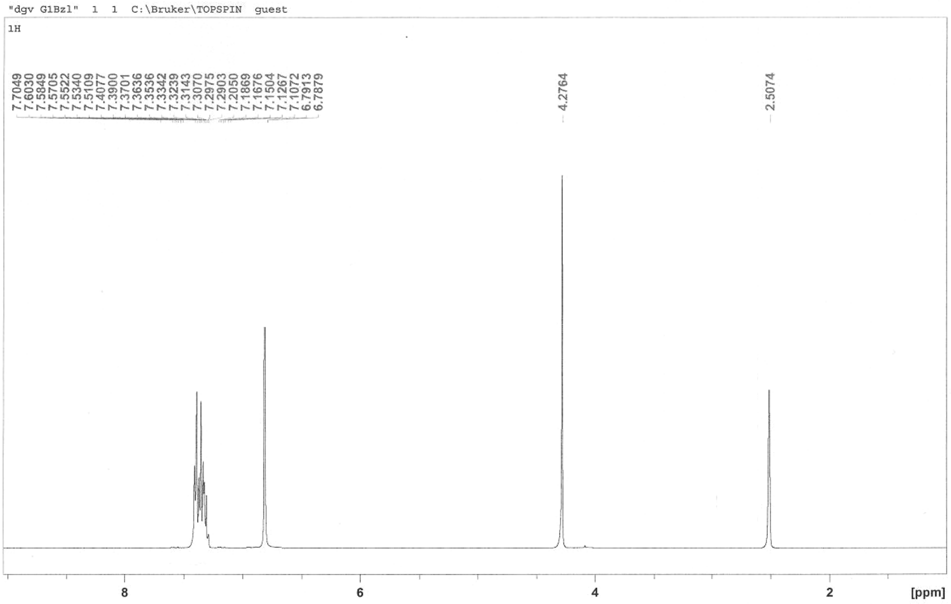

**Figure S5.** $^{1}$H NMR for **2** in DMSO-$d_6$

)

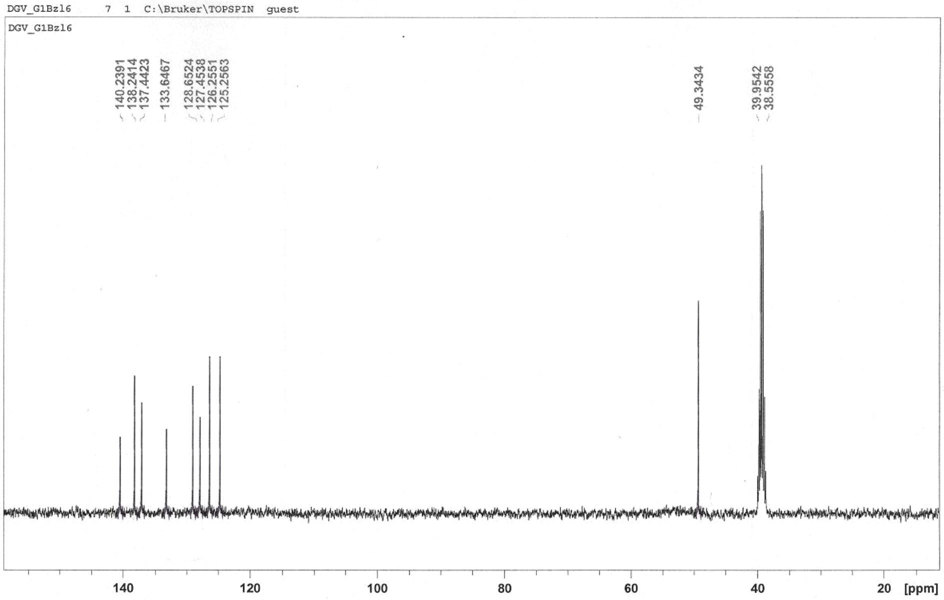

**Figure S6.** $^{13}$C NMR for **2** in DMSO-$d_6$

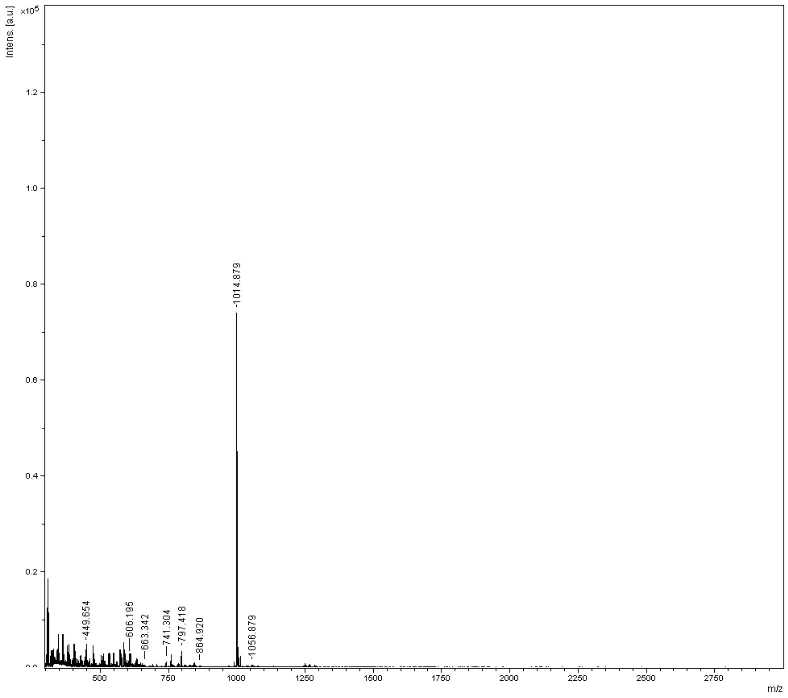

**Figure S7.** MALDI-TOF for **2** (DHB matrix; 5 mg/ml)

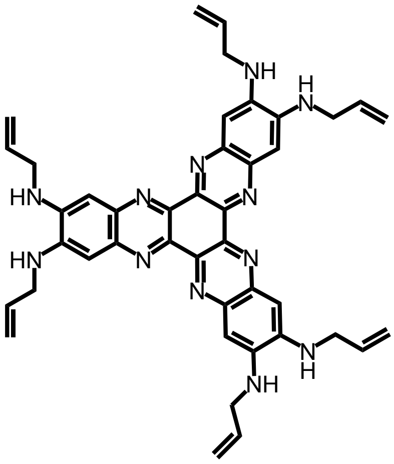

### 2.4 2,3,8,9,14,15-hexaallyldiquinoxalino[2,3-a:2',3'-c]phenazine-2,3,8,9,14,15-hexaamine (3):

To a 10 mL reaction vial was added G1 (30 mg, 0,06 mmol) and allyl bromide (12 equiv, 62 µL, 0,72 mmol) followed by 0.5 mL of water miliQ®. The closed vessel was heated and stirred in CEM Discover reaction cavity for 30 min at 150 ºC. Then the reaction vessel was rapidly cooled at 60 ºC. Upon cooling, the mixture was diluted with water (5 mL), neutralized with $NaHCO_3$, and extracted with EtOAc (3 x 10 mL); the organic phase was evaporated under reduced pressure, and the residue was purified by flash silica gel column chromatography (10% EtOAc in *n*-hexane as eluent). Drying for 48 h (under vacuum, 5-10 mmHg, 60-80 ºC) afforded a blue-dark solid as pure product (40 mg, 93%).

**Aspect**: blue-dark solid
**$^1$H NMR (400 MHz, *d6*-DMSO, δ ppm):** 4.08 (12H, d, J=Hz), 5.10-5.20 (6H, dd, $J_1$=Hz, $J_2$=Hz), 5.33 (6H, d, J=Hz), 5.85-6.10 (6H, m), 7.01 (6H, s)
**$^{13}$C NMR (100 MHz, *d6*-DMSO, δ ppm):** 46.58, 117.89, 128.16, 133.42, 135.00, 137.10, 138.42
**FT-IR (EtOH)**: 3194, 2982, 2884, 2198, 1413, 1218, 1198, 1134, 736, 659 cm$^{-1}$
**MS MALDI-TOF (*m/z* %)**: 714.44 [M$^+$]
**Elemental analysis:** for $C_{42}H_{42}N_{12}$: 715.37 g/mol. Calcd (%): C: 70.57, H: 5.92, N: 23.51. Found (%): C: 70.77, H: 6.23, N: 23.63.

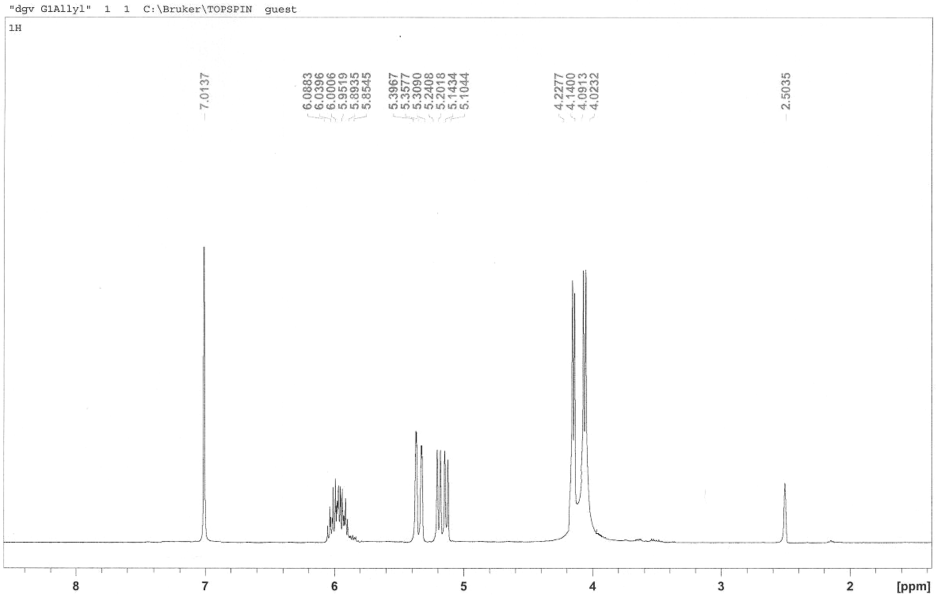

**Figure S8.** $^{1}$H NMR for **3** in DMSO-$d_6$

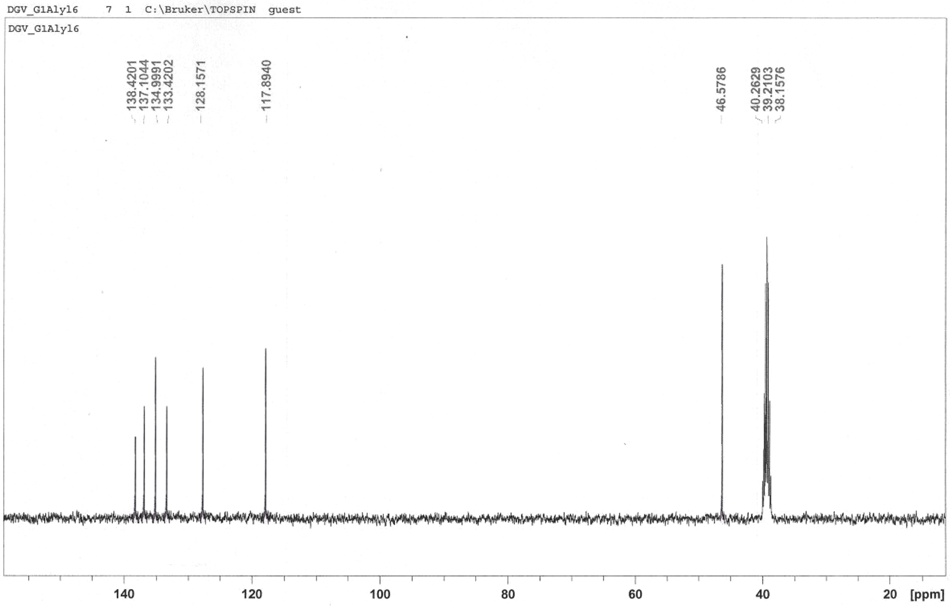

**Figure S9.** $^{13}$C NMR for **3** in DMSO-$d_6$

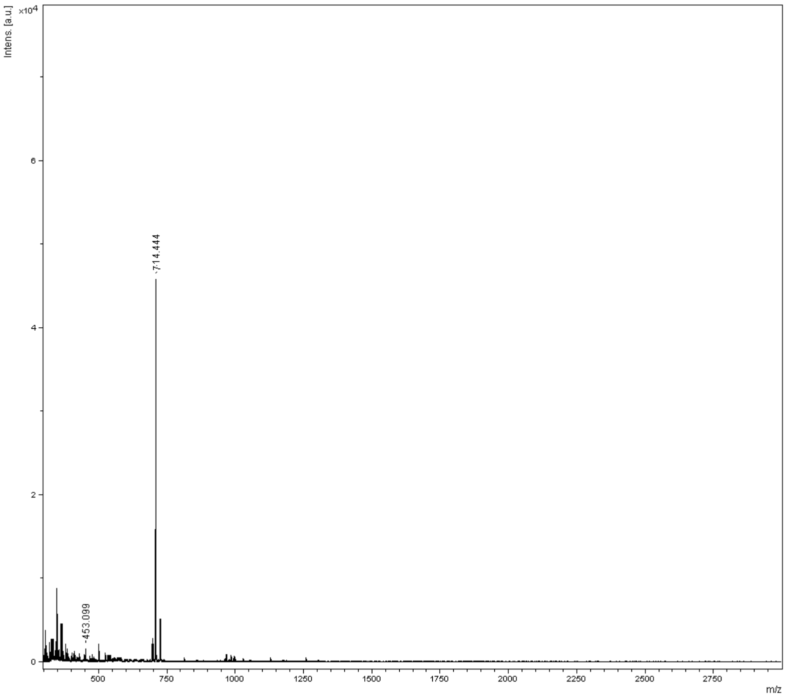

**Figure S10.** MALDI-TOF for **3** (DHB matrix; 5 mg/ml)

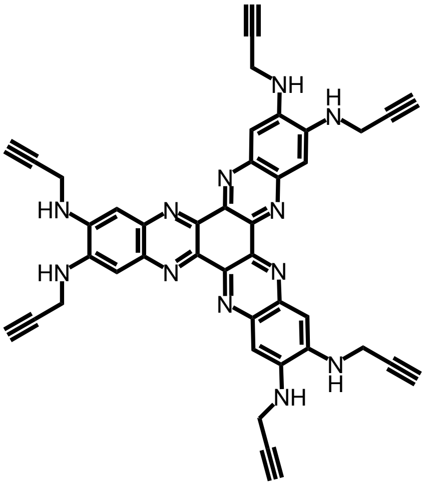

## 2.5 2,3,8,9,14,15-hexa(prop-2-ynyl)diquinoxalino[2,3-a:2',3'-c]phenazine-2,3,8,9,14,15-hexaamine (4):

To a 10 mL reaction vial was added G1 (30 mg, 0,06 mmol) and propargyl bromide 80% (12 equiv, 50 µL, 0,72 mmol) followed by 0.5 mL of water miliQ®. The closed vessel was heated and stirred in CEM Discover reaction cavity for 30 min at 150 ºC. Then the reaction vessel was rapidly cooled at 60 ºC. Upon cooling, the mixture was diluted with water (5 mL), neutralized with $NaHCO_3$, and extracted with EtOAc (3 x 10 mL); the organic phase was evaporated under reduced pressure, and the residue was purified by flash silica gel column chromatography (20% EtOAc in *n*-hexane as eluent). Drying for 48 h (under vacuum, 5-10 mmHg, 60-80 ºC) afforded a black solid as pure product (36 mg, 85%).

**Aspect**: black solid
**$^1$H NMR (400 MHz, *d6*-DMSO, δ ppm):** 2.68 (6H, s), 3.71 (12H, s), 6.69 (6H, s)
**$^{13}$C NMR (100 MHz, *d6*-DMSO, δ ppm):** 30.55, 73.76, 80.53, 126.79, 132.90, 137.48, 138.57
**FT-IR (EtOH)**: 3258, 3093, 2921, 2260, 1471, 1274, 1237, 1223, 734, 668 cm$^{-1}$
**MS MALDI-TOF (*m/z* %)**: 702.25 [M$^+$]
**Elemental analysis:** for $C_{42}H_{30}N_{12}$: 703.77 g/mol. Calcd (%): C: 71.78, H: 4.30, N: 23.92. Found (%): C: 71.87, H: 4.39, N: 23.80.

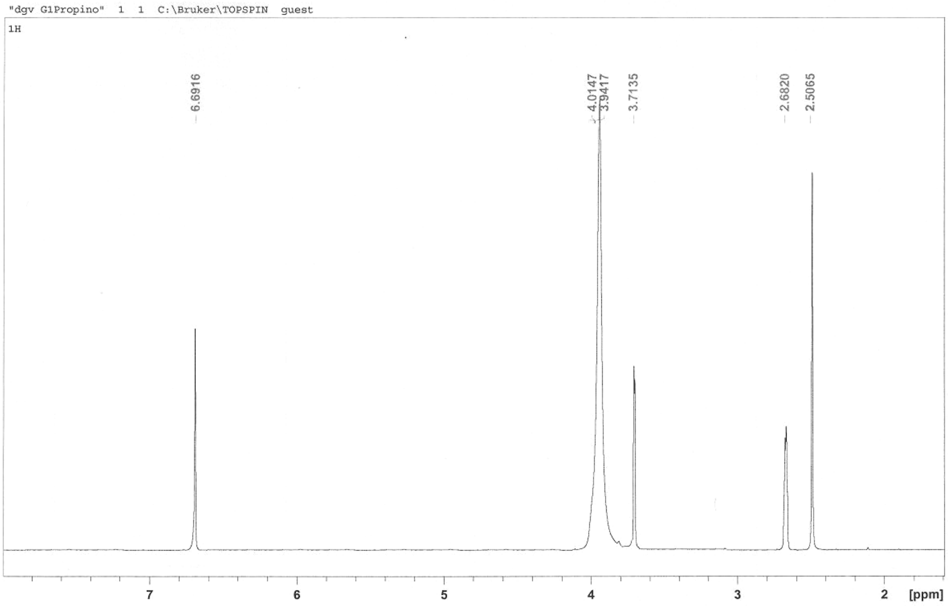

**Figure S11.** $^1$H NMR for **4** in DMSO-$d_6$

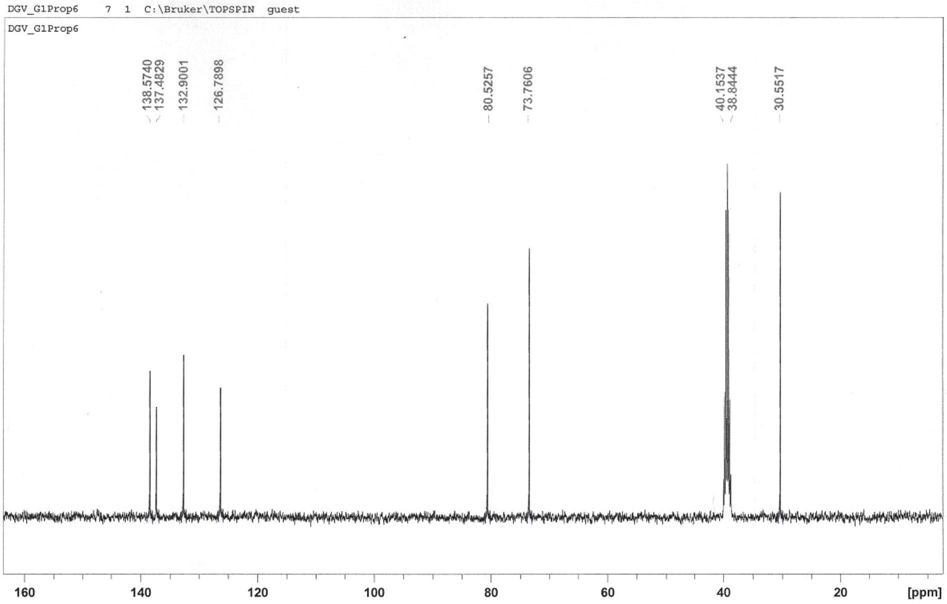

**Figure S12.** $^{13}$C NMR for **4** in DMSO-$d_6$

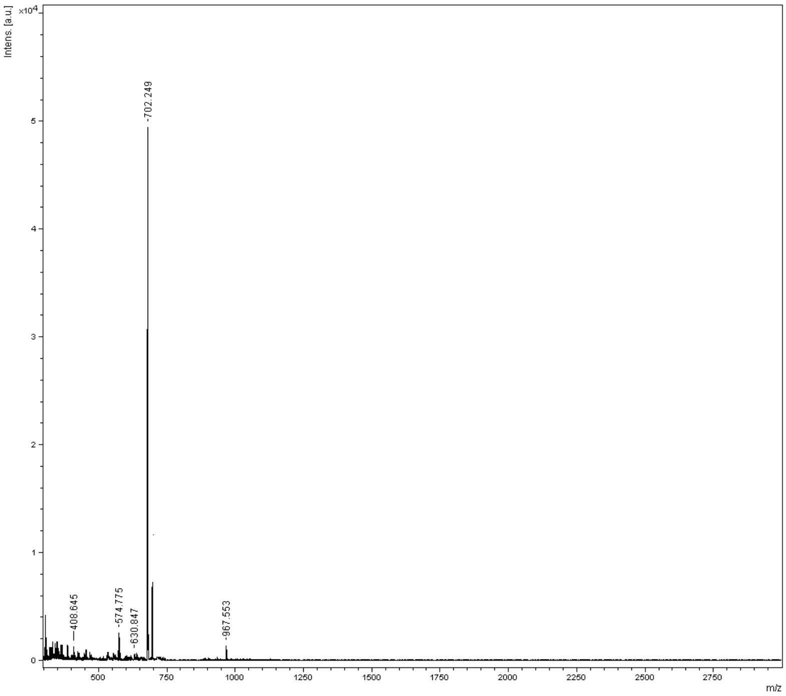

**Figure S13.** MALDI-TOF for **4** (DHB matrix; 5 mg/ml)

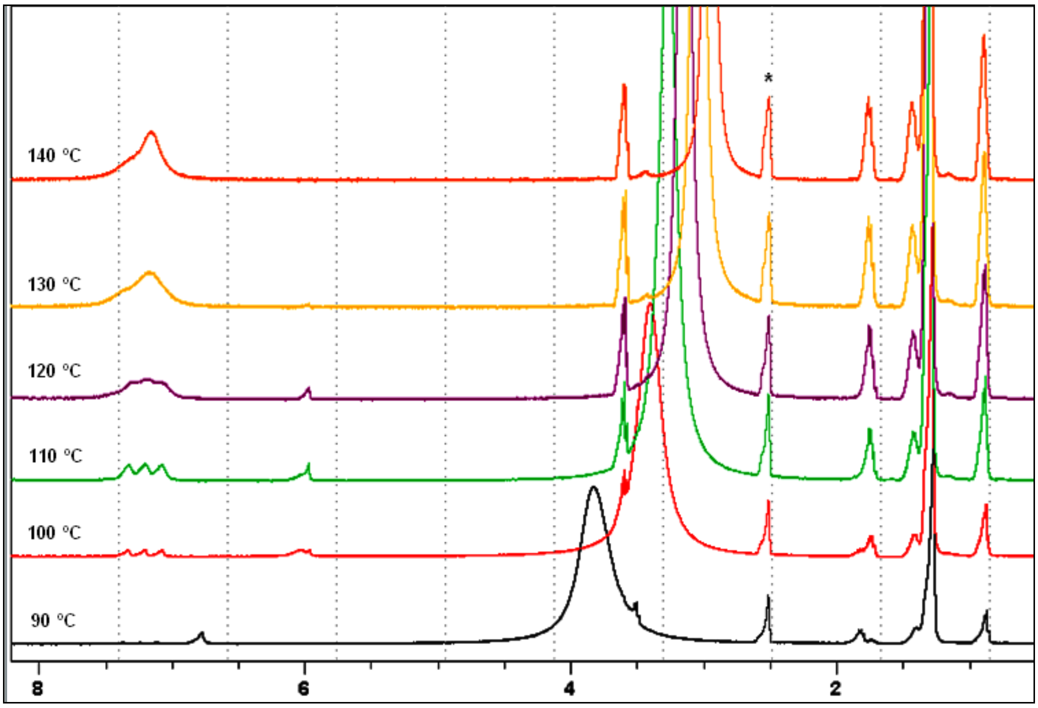

**Figure S14.** $^1$H NMR temperature-dependent for **1** (0.36 wt% ; $T_{gel}$ = 119 ºC) in DMSO-$d_6$ (asterisk signal)

## 3. Gelation Ability, $T_{gel}$, and Digital Photographs of the Gels.

At RT, the compound **1** and **2** were found to be sparingly soluble in DMSO, DMF, acetone, toluene, benzene and *n*-hexane. Upon heating the solid fully dissolved and the formation of the gel was observed upon cooling. Interestingly, no gelation was observed when amide derivates were used.[13] In addition, the availability of the free -$NH_2$ groups is not mandatory for the self-assembly process leading to gelation, although they are the responsible of columnar aggregation.[13]

The stable gels were homogeneous and can be stored at room temperature without disruption or precipitation at least over a month. Translucid gels were formed in a variety of solvents at the critical gelation concentration as indicated in Table S1 although most of these gels turned opaque or turbid at higher concentrations of organogelator (Figure S14). The presence overlapped fibers may promote the formation of microparticles and account for the opacity of the gels. In other hand, compacted fibrous character of the sheets in some gels could indicate some confined crystallinity.

**(A)** **(B)**

**Figure S14.** Digital photographs of the organogels prepared at different concentrations of LMWOG **1** and **2**: **(A)** 1.10 wt% of **2** in toluene (*left*) and 0.36 wt% of **1** in DMSO (*right*); **(B)** 2.5 wt% of **2** in toluene.

Table S1 shows the complete list of solvents tested for gelation. No gel formation was observed for the cases marked as “S” even at low temperature (< 5 ºC). As expected, $T_{gel}$ values of the gels increased with the concentration of the LMWOG **1** (Figure S15, Phase diagram for acetone-gel).

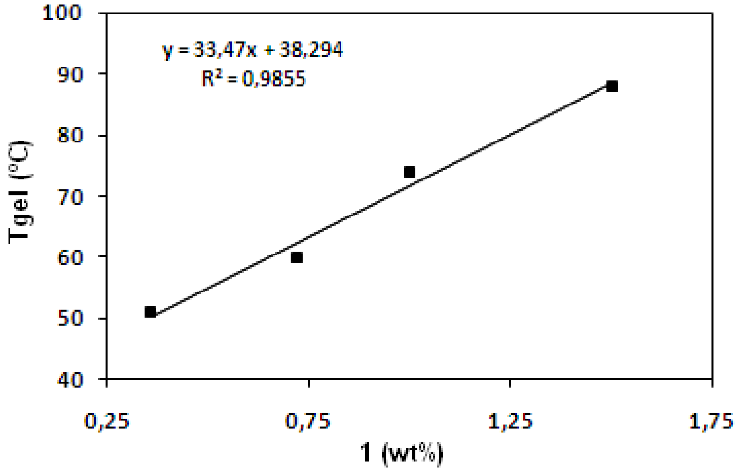

**Figure S15.** Gel melting temperatures as determined with the *dropping ball* method for gels in acetone at different concentrations of **1**.

**Table S1** Physical data for gels of **1** (green) and **2** (red) in various solvents.

| Solvent | cgc **1** (wt%)[a] | Phase[b] | $T_{gel}$ (ºC)[c] | Appearance |
|---|---|---|---|---|
| 2- Propanol | – | S | – | – |
| Chlorobenzene | – | S | – | – |
| Chloroform | – | S | – | – |
| Dichloromethane | – | S | – | – |
| Dimethylformamide | 1.10 | G | 133 | translucid |
| Dimethylsulfoxide | 0.36 | G | 119 | translucid |
| Ethanol | – | S | – | – |
| *p*-Xylene | – | S | – | – |
| Tetrahydrofurane | – | I | – | – |
| Ethyl Acetate | – | S | – | – |
| Ethanol | – | S | – | – |
| Acetone | 1.40 | G | 51 | translucid |
| Toluene | 0.50 | G | 80 | translucid |
| *n*-Hexane | 1.78 | G | 70 | translucid |
| Benzene | – | S | – | – |
| Perfluorohexane | – | V | – | – |
| Acetonitrile | – | P | – | – |
| Water | – | I | – | – |

| Solvent | cgc **2** (wt%)[a] | Phase[b] | $T_{gel}$ (ºC)[c] | Appearance |
|---|---|---|---|---|
| 2- Propanol | – | S | – | – |
| Chlorobenzene | – | V | – | – |
| Chloroform | – | S | – | – |
| Dichloromethane | – | S | – | – |
| Dimethylformamide | – | S | – | – |
| Dimethylsulfoxide | – | V | – | – |
| Ethanol | – | S | – | – |
| *p*-Xylene | – | V | – | – |
| Tetrahydrofurane | – | P | – | – |
| Ethyl Acetate | – | S | – | – |
| Ethanol | – | S | – | – |
| Acetone | – | S | – | – |
| Toluene | 1.1 | G | 107 | translucid |
| *n*-Hexane | – | P | – | – |
| Benzene | 0.5 | G | 58 | translucid |
| Perfluorohexane | – | I | – | – |
| Acetonitrile | – | S | – | – |
| Water | – | I | – | – |

[a] The cgc is the critical gelation concentration at which gelation was observed to restrict the flow of the medium. [b] Abbreviations: G = stable gel (> 1 month); S = solution; P = precipitation; V = viscous; I = Insoluble upon heating. [c] Determined by the dropping ball method..

## 4. Representative DSC Thermogram.

**Table S2** Thermodynamic parameters for gels of **1**.

| **Solvent** | **weight of gel (mg)** | $T_{gel}$(ºC) [a] | $T_{gel}$ (ºC) [b] | ΔH (J/g) [c] |
|---|---|---|---|---|
| Dimethylformamide | 6.2 | 133 | 134-135.5 | 0.20 |
| Dimethylsulfoxide | 7.1 | 119 | 118.5-120.5 | 0.42 |
| Acetone | 8.9 | 51 | 50-52 | 0.38 |
| Toluene | 4.5 | 80 | 79-82 | 0.12 |
| *n*-Hexane | 8.6 | 70 | 68-70 | 0.27 |

[a] Gel-sol transition temperature at c.g.c. determined by the "dropping ball method" (ramping rate < 2 ºC). [b] The first value corresponds to the onset of the endothermic peak by DSC and the second value to the maximum. [c] Enthalpic change. The estimated error for the $T_{gel}$ obtained by the "dropping ball method" and DSC were ± 1 ºC and ± 3 ºC respectively.

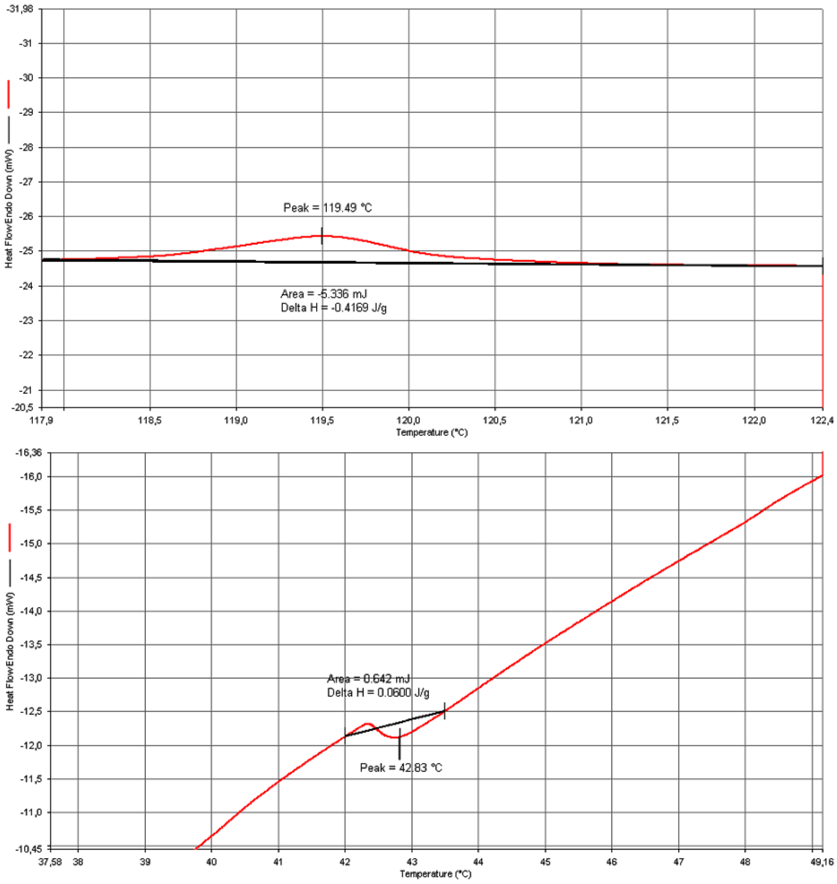

**Figure S16.** DSC spectrum (heating-cooling cycle) of the organogel prepared from 0.36 wt% of **1** DMSO ($T_{gel}$ = 119 ºC).

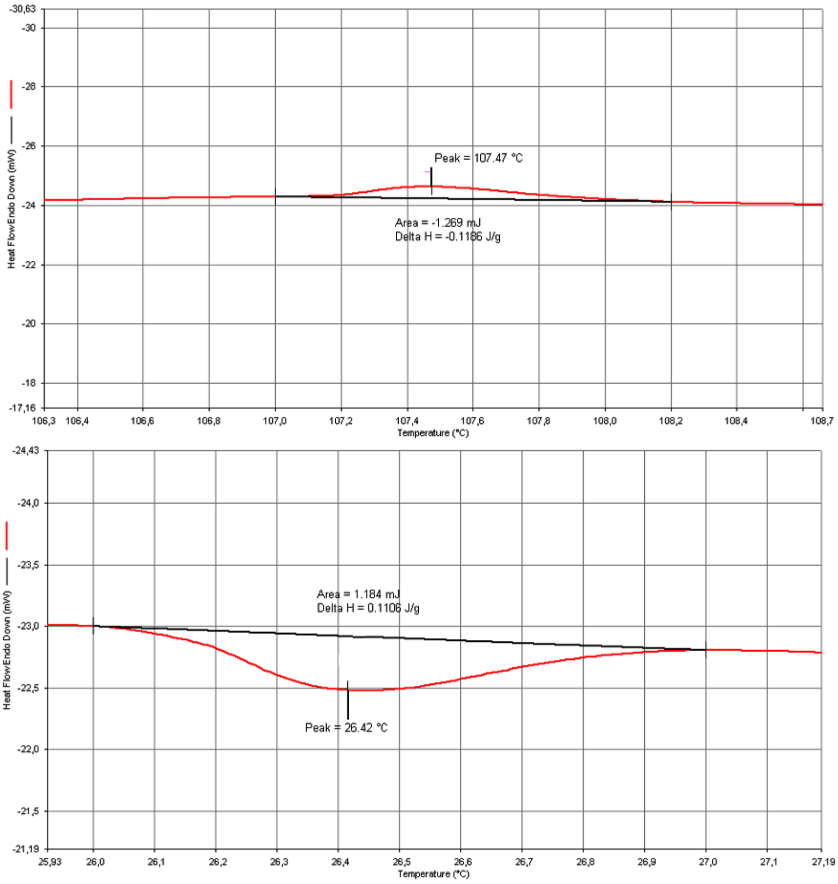

**Figure S17.** DSC spectrum (heating-cooling cycle) of the organogel prepared from 1.10 wt% of **2** toluene ($T_{gel}$ = 107 ºC).

## 5. Typical FT-IR Spectra of Gel Samples.

IR spectra of gels were obtained by depositing the gel on NaCl disk and recording the spectrum directly operating at 8 $cm^{-1}$ resolution with 40 scans. Corrections were made for the solvents. In general, the NH group undergoes hydrogen bonding and shifts to lower frequency. The fact that IR spectra change when the gel is broken (consistent with the $T_{gel}$) indicates that the gel-to-sol transition is induced by breaking hydrogen bonds and van der Waals interactions (data not shown). In addition to hydrogen bonding, for which the NH groups are crucial, $\pi$-$\pi$ stacking may also play significant roles in promoting the efficient organization of **1** into aggregates and fibers.

Typical FT-IR spectra are shown in Figure S18:

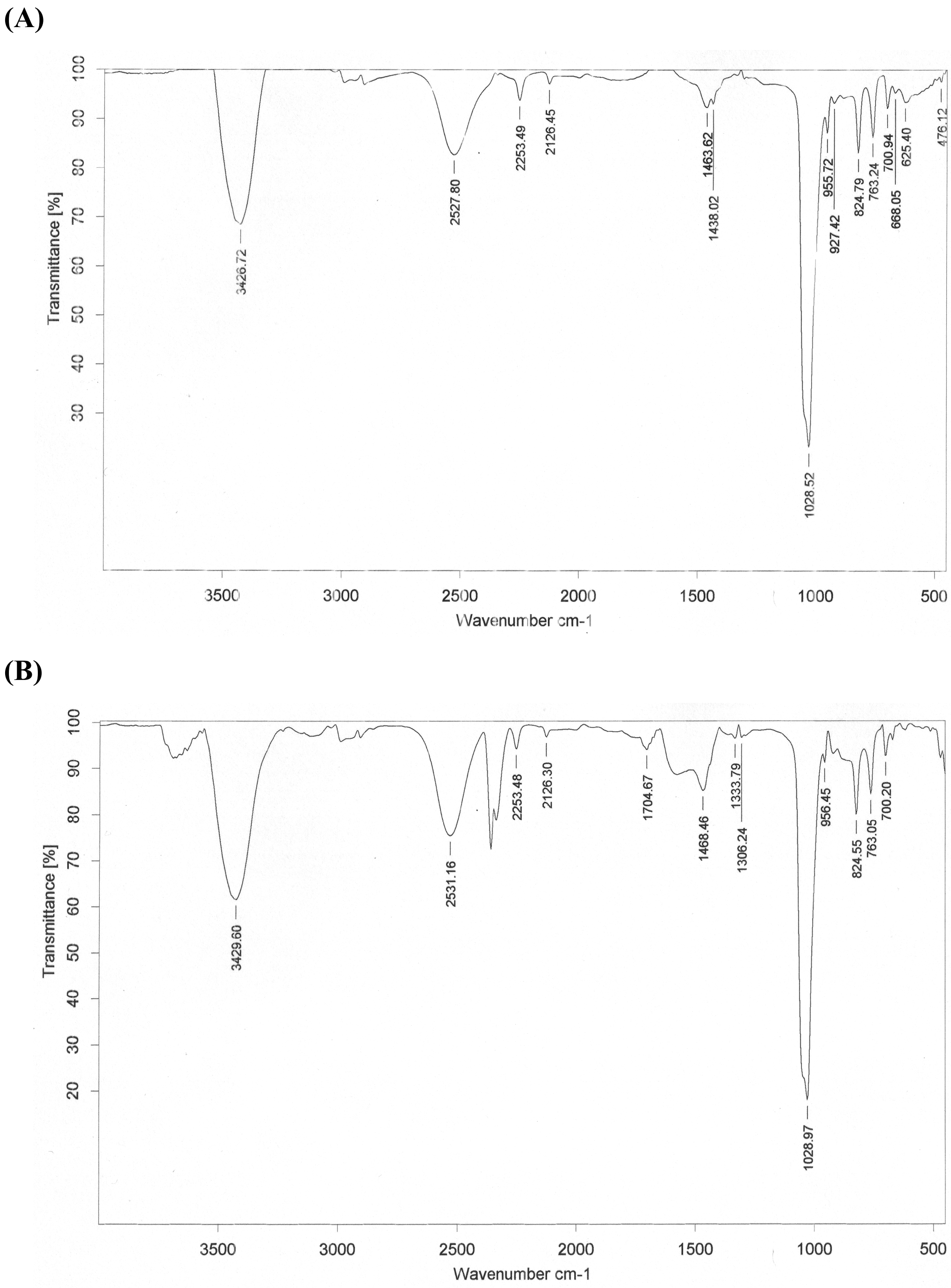

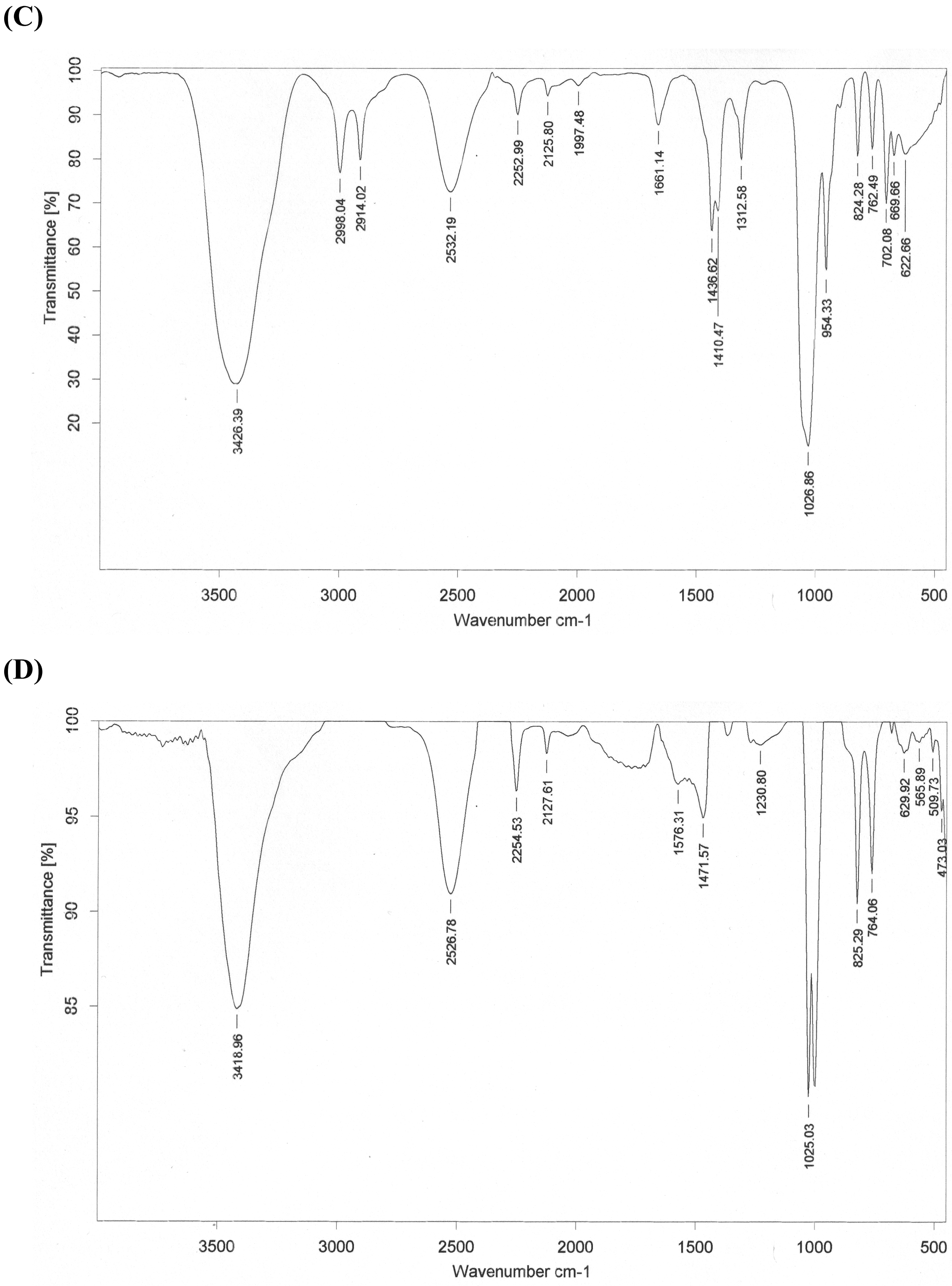

**Figure S18.** (A) FT-IR spectra for **1** (solid state), (B) **1**-containing organogel (0.36 wt% in DMSO), (C) **1**-containing organogel (1.40 wt% in acetone), (D) **1**-containing solution (in dichloromethane).

## 6. TEM Pictures.

A change in the solvent and/or the concentration has a considerable effect on the morphology of the fibers (length, shape and diameter) as evidenced from the electronic micrographs. A representative collection of such images are given bellow:

**a)** 0.36 wt% LMWOG **1**; solvent = dimethylsulfoxide; $T_{\text{gel}} = 119$ °C

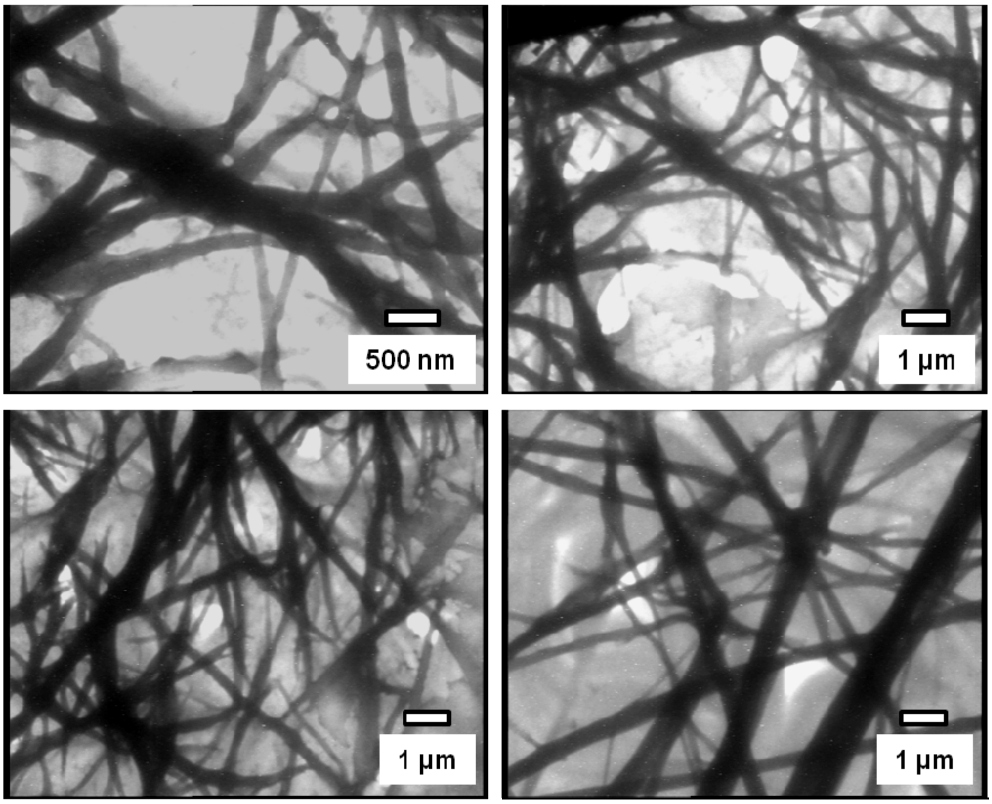

**b)** 1.10 wt% LMWOG **2**; solvent = toluene; $T_{gel}$ = 107 °C

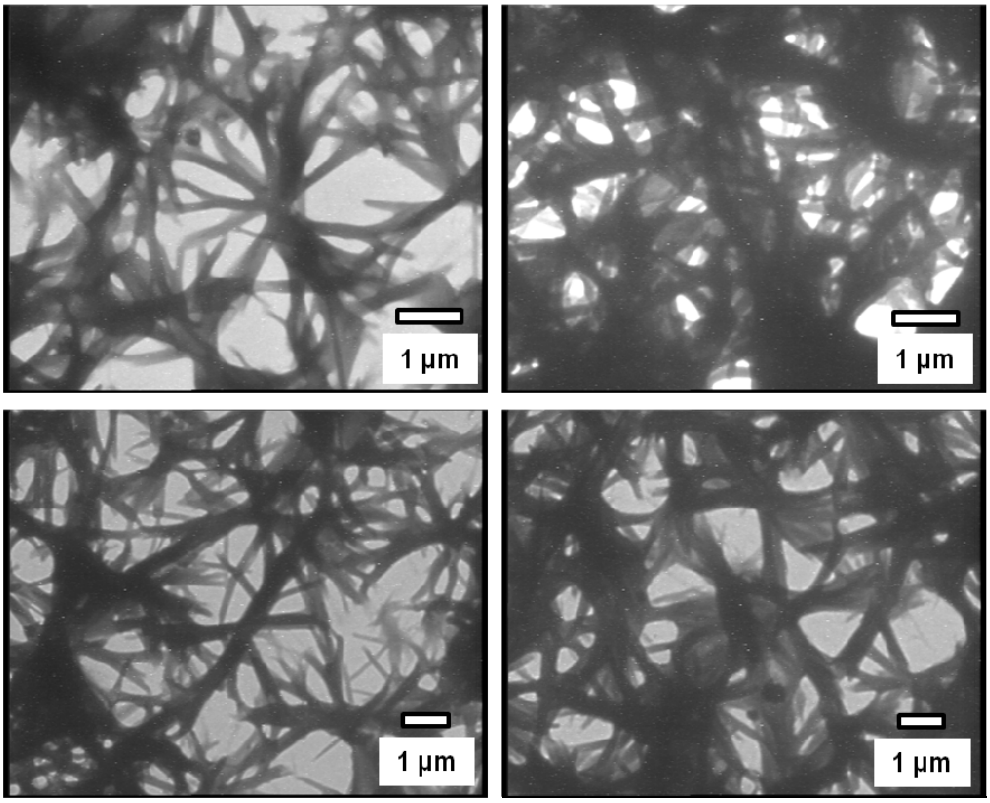

**c)** 1.0 wt% LMWOG **1**; solvent = dimethylsulfoxide.

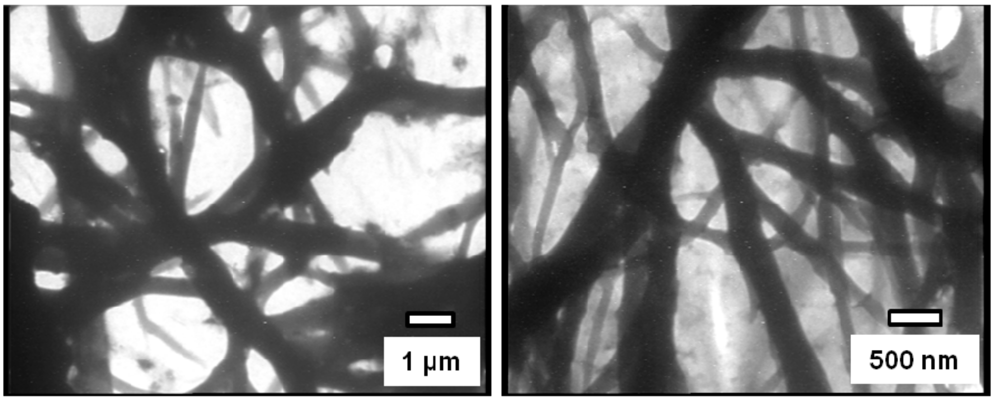

**d)** 0.36 wt% LMWOG **1**; solvent = dimethylsulfoxide; Detail of twisted (black arrows) structure formed by **1**. The lenght of the white bar (inset) across the thinnest fiber is 25 nm.

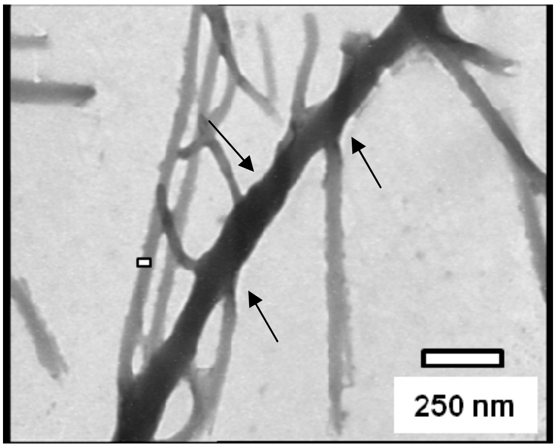

## 7. SEM Pictures.

**a)** 0.36 wt% LMWOG **1**; solvent = dimethylsulfoxide.

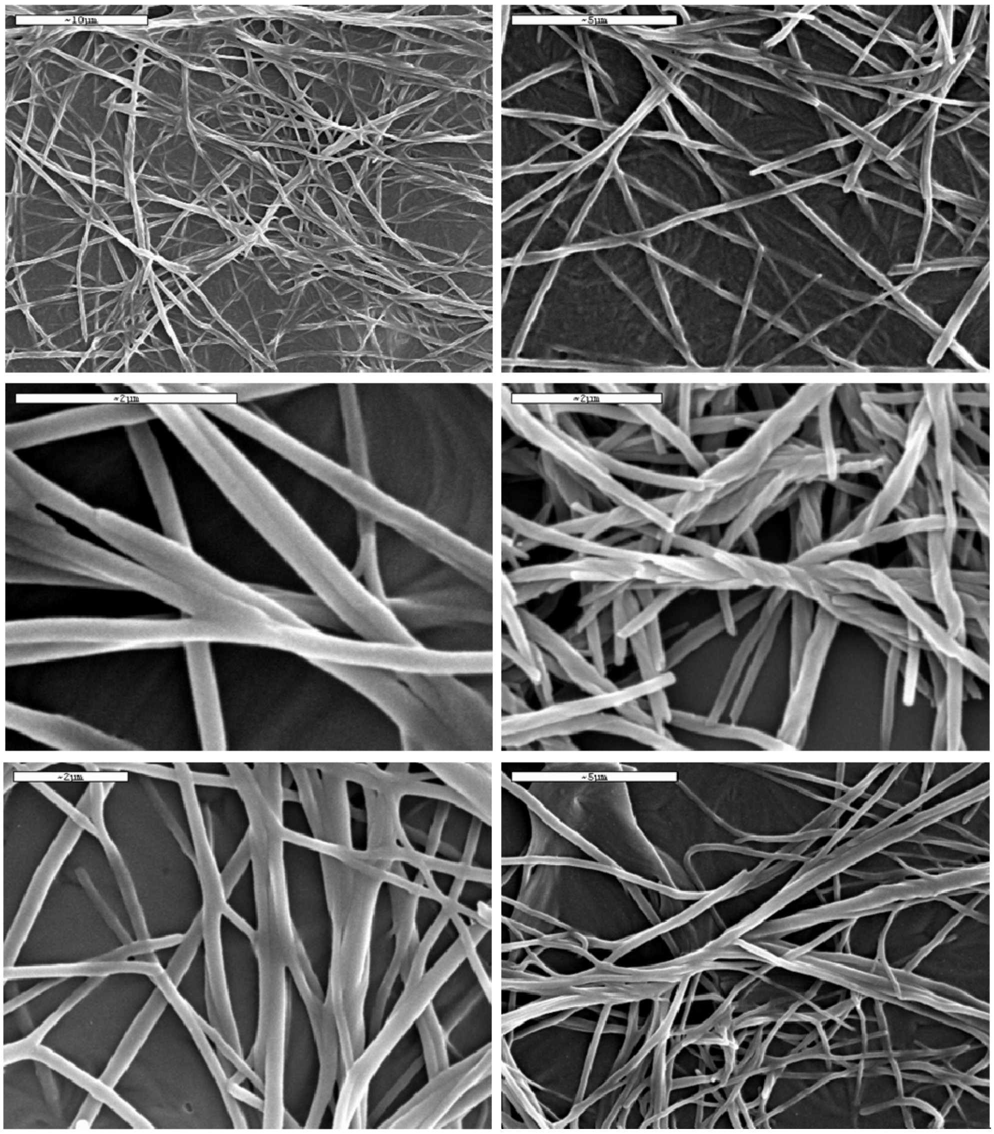

**b)** 1.10 wt% LMWOG **2**; solvent = toluene.

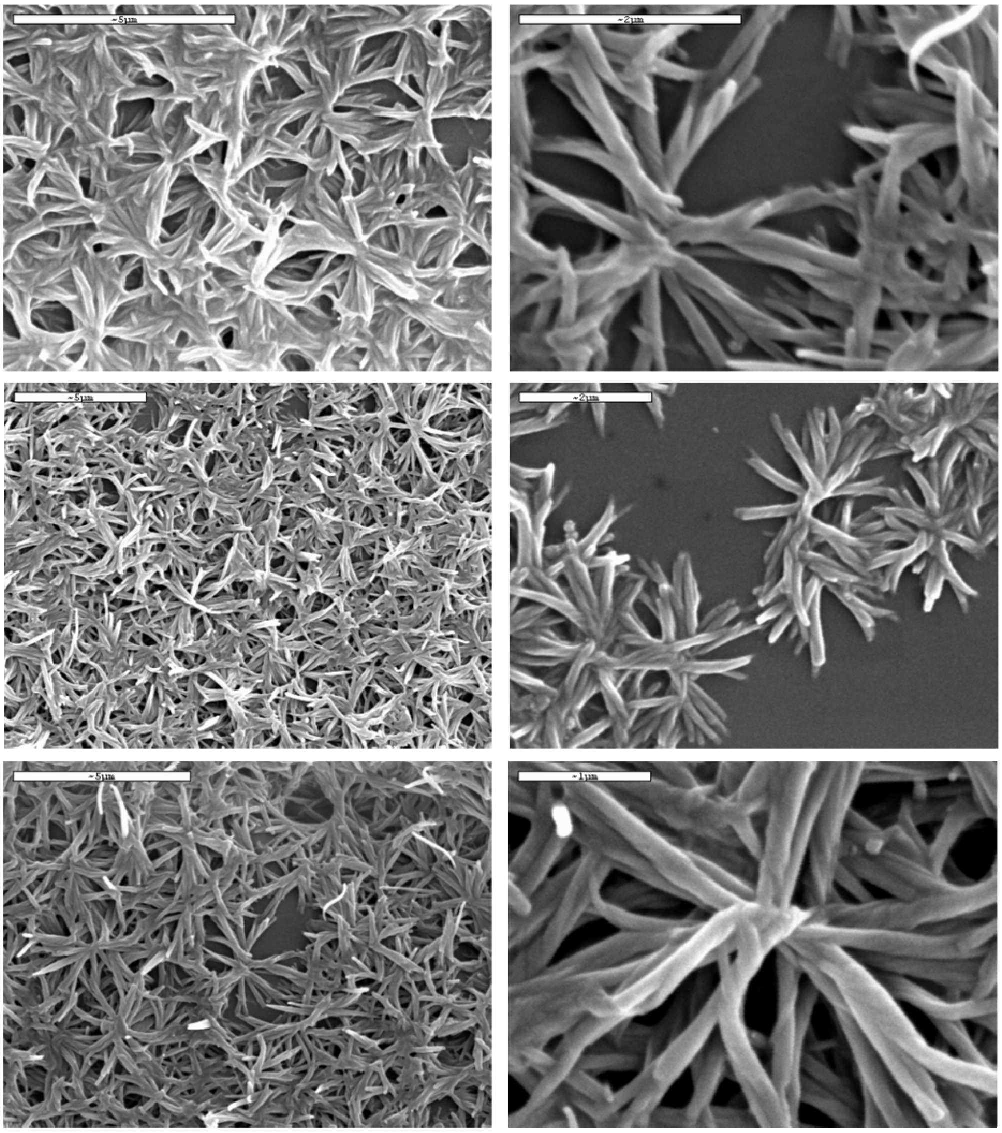

## 8. Fluorescence of compound 2 in solution

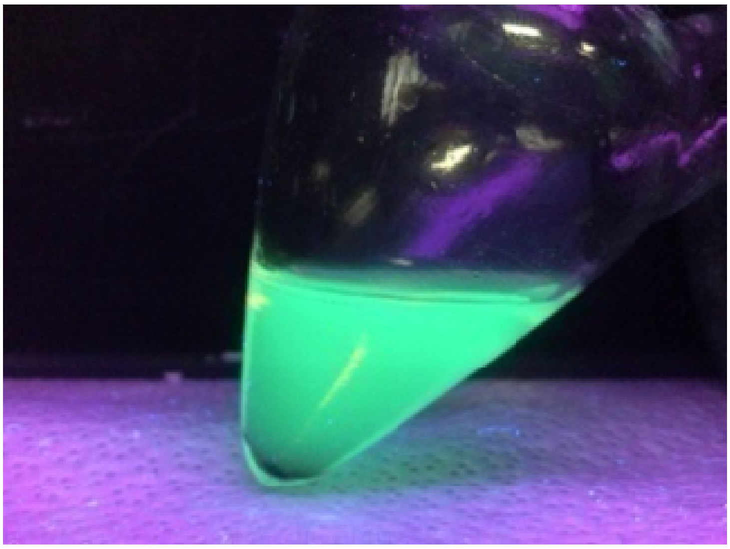

Fluorescence of compound 2 in solution at 365 nm in benzene (high dilution)

## 9. AFM Pictures.

**a)** 0.36 wt% LMWOG **1**; solvent = dimethylsulfoxide.

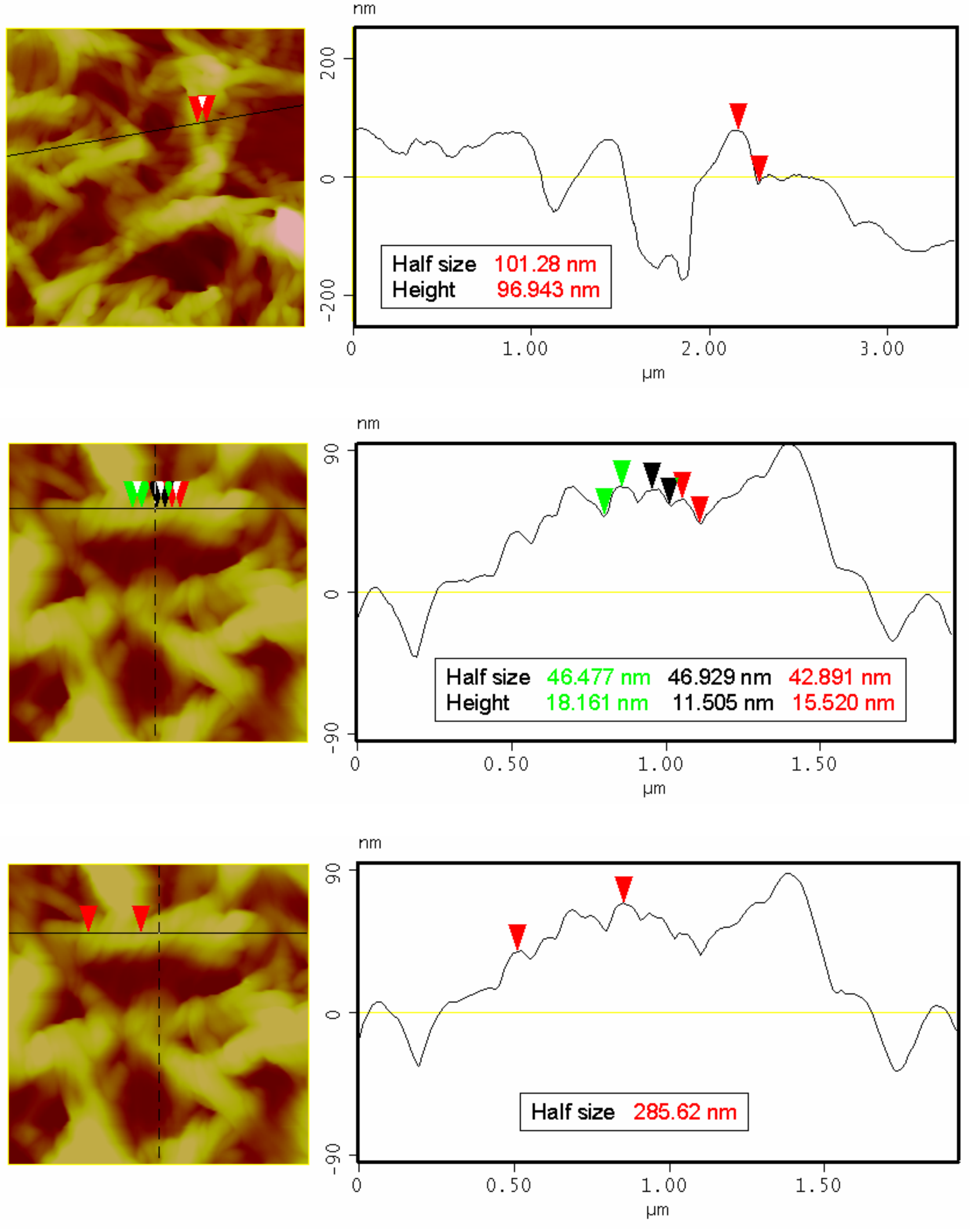

**b)** 1.10 wt% LMWOG **2**; solvent = toluene.

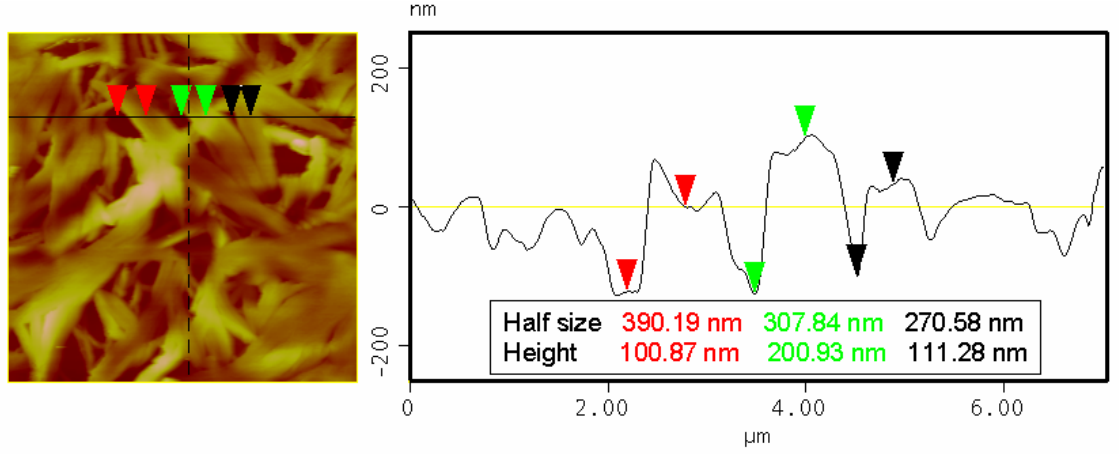

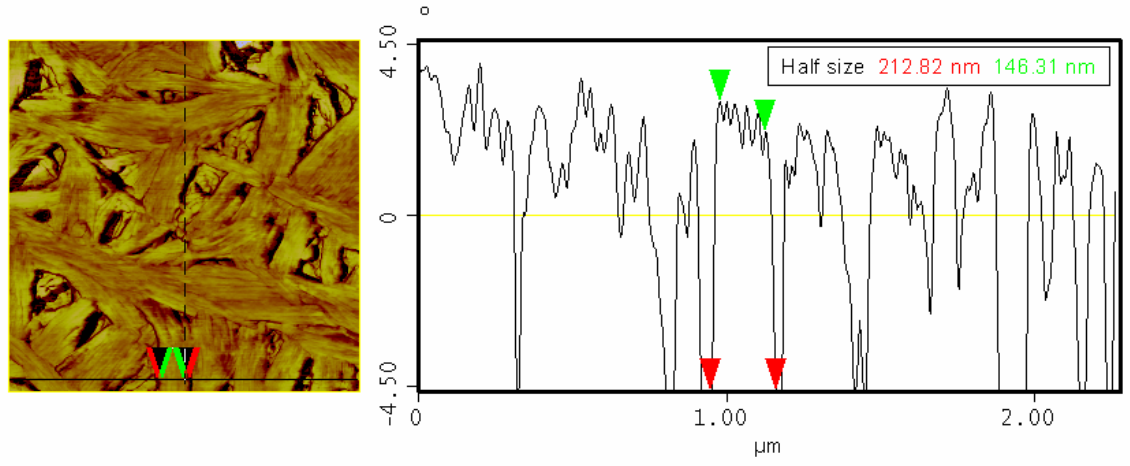

## 10. Polarized Optical Microscopy (POM)

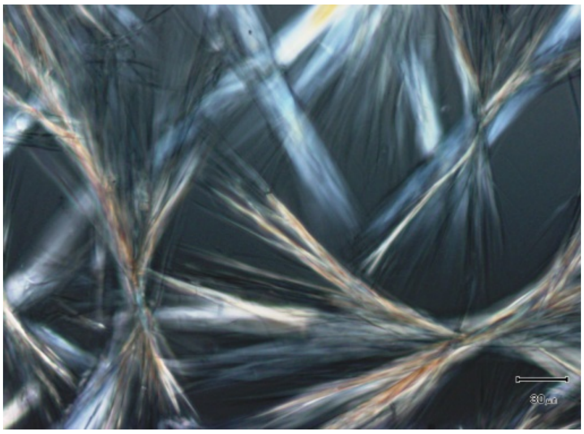

**Figure S19.** Image of POM (heater-plate coupled) of **2** in toluene (transition *sol-to-gel* cooling-heating cycle; rate: 5 $^{o}$C/min)

## 11. Optimized geometry

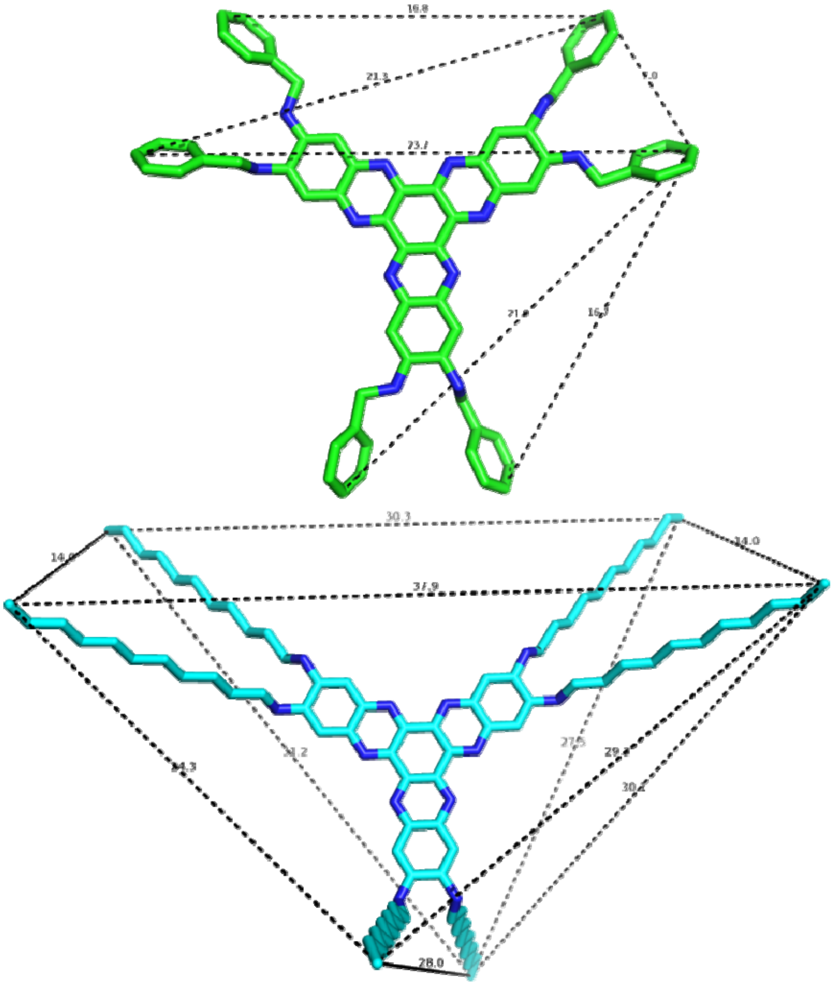

**Figure S20.** Calculated minimized structures (HF/3-21G) of gelator **1** (down) and **2** (up) (distances in Å).

## 11. Hypothetic model

We suggest a stacking model for the HATNA moieties (**1** and **2**) through van der Waals interactions responsible for the formation of the organogels. As a consequence, the side chains are shifted towards the periphery of the core and thus may be responsible for the interactions with the solvent. The fibers further intertwine to generate hierarchically defined structures as documented by the microscopic techniques in this communication.

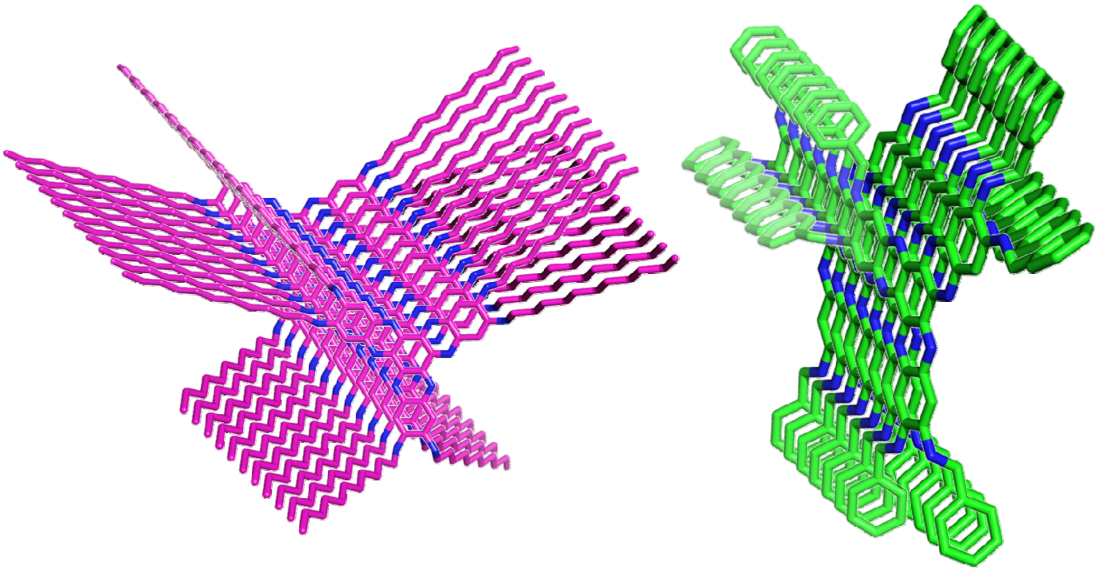

**Figure S21.** Hypothetical representation of self-assembly of gelators **1** (*left*) and **2** (*right*)

## 12. References y notes.

† Due to the limited space in the main paper for acknowledgments, the authors wish to thank also herein Dr. J.R. Hernández-Fernaud for assistance with MALDI-TOF measurements and Dr. Elisa Pérez-Sacau for modelling molecular. AGO acknowledges MEC for a predoctoral fellowship. DGV acknowledges to Prof. Fernando García-Tellado for supplying the microwave instrument and for his valuable input and shared interest in our work. DGV acknowledges to group of Prof. Antxón Santamaría for assistance in rheological measurements.

---

[1] W. L. F. Armarego, D. D. Perrin, Purification of Laboratory Chemicals, 4th ed., Butterworth–Heinemann, Oxford, 1996.

[2] A. Takahashi, M. Sakai, T. Kato, *Polym. J.* 1980, **12**, 335.